

Communications

SMART^{Wheels}: Development and Testing of a System for Measuring Manual Wheelchair Propulsion Dynamics

Kimberly T. Asato, Rory A. Cooper, Rick N. Robertson, and J. F. Ster

Abstract—The purpose of this project was to develop a system for dynamically sensing pushrim propulsion forces and torques and to collect kinetic data with the device. A system was developed to detect the forces and torques applied to the wheelchair pushrim, record, store, and process the measured data, and display the kinetic information for analysis. Ten adults, including four male wheelchair users, three ambulatory men, and three ambulatory women, pushed a wheelchair with the SMART^{Wheel} on a dynamometer while their kinematics were videotaped. The kinetic data collected with our wheel were correlated with stick figure representations of digitized kinematic data obtained through video analysis. The close agreement between the kinetic results and the Kinematic results provided a temporal validation of the ability of the wheel to detect forces and torques applied to the wheelchair pushrim. The recorded forces and torques were in agreement with previously reported magnitudes.

I. INTRODUCTION

Researchers have stated that there is a need for greater interdisciplinary interaction and coordination for developing instrumentation for furthering research on wheelchair pushrim propulsion [1]–[6]. This paper addresses the need for a tool which enables direct measurement of the forces and torques applied by the wheelchair user to the push rim. A pushrim force and torque sensing wheel is necessary to further the understanding of how forces generated by the individual are being directed and allow for interpretation related to optimizing efficiency, improving performance, identifying causes of injuries (such as carpal tunnel syndrome, elbow tendonitis, and shoulder rotator cuff injuries) and developing prevention techniques.

Van Der Woude *et al.* have reported on an ergometer which detected torque by way of a force transducer located in the wheel center and attached to what is referred to as the "wheel/hand rim construction" [7]. The ergometer was adjusted for each subject's anthropometric measurements. Data were sampled at 100 Hz for 7.5 s periods with a digital filter cutoff frequency of 10 Hz. Mean and peak torque increased with mean velocity, a maximum mean peak torque of 31 Nm occurred at 1.27 Ms. Torque curves of inexperienced subjects showed an initial negative deflection and a dip in the rising portion of the curve. Torque curves were reported to be in agreement with results of previous investigations [8]–[10].

A Kistler piezoelectric force platform was used by Tupling *et al.* [11] to measure the force generated during initiation of wheelchair movement. They studied the force generated using the grab and strike start techniques and examined its relation to arm strength of paraplegics of varying physical activity and lesion levels. They

Manuscript received May 18, 1993; received November 28, 1993. This work was supported in part by grants from California State University Sacramento Research Assigned Time Program, the Rehabilitation Services Administration under grant number H129E00005, and in part by the U. S. Department of Veterans Affairs, Rehabilitation Research and Development Center, Edward Hines Jr. Hospital under grant number VA578-92-2-105-0250.

The authors are with the Human Engineering Laboratory, Department of Biomedical Engineering, California State University, Sacramento, CA 95819-6019.

IEEE Log Number 9213162.

concluded that the grab start was a more effective method of initiating movement than the strike start and that impulse generation is related to muscle strength [6],[11].

Brauer and Hertig [12] measured the static torque produced on push rims which were rigidly restrained by springs and mounted independent of the tires and rims of the wheelchair. The spring system was adjustable for the subject's strength. The wheels were locked in a fixed position. Torque was measured using slide-wire resistors coupled to the differential movements between the pushrim and wheels and recorded using a strip chart recorder. Subjects were asked to grasp the pushrim at six different test positions—10, 0, 10, 20, 30, and 40° relative to vertical) and to use maximal effort to turn both wheels forward. Male subjects (combined ambulatory and wheelchair user) produced torques of 27.9 to 46.6 Nm and female subjects produced torques of 17.1 to 32.1 Nm [12]. Grip location, handedness, grip strength, and how well the test wheelchair fit the anthropometric measurements of the individual affected the torque generated. Problems encountered were slipperiness of the push rims due to a polished finish and limited contact due to the small diameter of the pushrim tubing (12.7 mm or 1/2 in). The use of one wheelchair for all subjects presented the problem of variations due to inappropriate fit for some individuals.

Brubaker, Ross, and McLaurin [13] examined the effect of horizontal and vertical seat position (relative to the wheel position) on the generation of static pushrim force. Force was measured using a test platform with a movable seat and strain gauged beams to which the push rims were mounted. Pushing and pulling forces were recorded using a strip chart recorder. Static force was measured for four grip positions (-30, 0, 30, and 60°) with various seat positions. Pushrim force ranged from approximately 500–750 N and varied considerably with seat position and rim position [13].

Strauss *et al.* reported that calibration of their dynamic system revealed problems in terms of linearity and drift [14],[15]. The sensitivity and linearity of their system only permitted the measurement of torque. A brief description of a second prototype was reported to employ an AMTI six degree of freedom strain gauge based force transducer, 3 AD1B31AN strain gauge signal conditioners, and AD8471JN amplifiers for measuring force. It was stated that their system transfers data from the sensor to a computer either through a direct wire link or via a microprocessor based (Intel 80C196KB) digital FM transmitter-receiver system.

Cooper and Cheda [3],[4] described a system for dynamically measuring racing wheelchair pushrim propulsion forces and torques. The device consisted of a slotted disc upon which various sized pushrims could be mounted. The disc was attached to the hub via three beams, each instrumented with two strain gauge bridges. The design for the electronic signal processing included the use of transistor temperature compensation, amplification, pulse amplitude modulation, frequency division multiplexing using a summer, and a mercury slip ring. It was proposed that the signal from the slip ring could be stored using a recorder for later processing with a microcomputer or could be interfaced to a data acquisition board for real time applications [3], [16]. Results were not reported using this initial design. The device proposed in the present study is the next generation in this particular development.

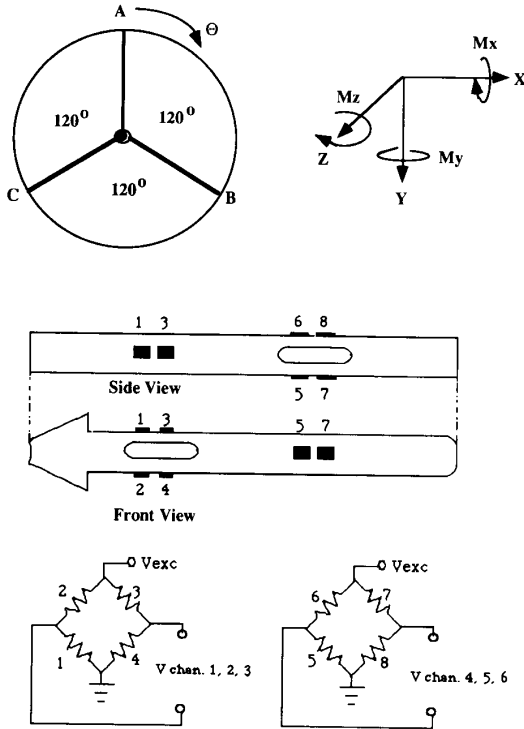


Fig. 1.

II. THE SMART^{Wheel} SYSTEM

The SMARTWheel is a pushrim force and torque sensor which was designed, fabricated, calibrated, and tested through a pilot study.

This system design is based on equations for a three-beam (120° apart) system for pushrim force and torque detection utilizing strain gauges. The following is the mathematical analysis of the measurements necessary to calculate F_x , F_y , F_z , M_x , M_y , and M_z for a six degree of freedom wheel. The beams are referred to as beams A, B, and C, the beams were instrumented to measure F_x , F_y , and M_z only (Fig. 1).

Channels 1, 2, and 3 measure beam deflection in the plane of the wheel. The measured signals for the three channels are referred to as V_1 , V_2 , V_3 and k_1 , k_2 , and k_3 are the calibration constants for the three channels, respectively. The position of beam A with respect to top dead center is given by θ , where $0^\circ < \theta \leq 360^\circ$. The distance between the hub and the point at which the pushrim attaches to the beam is given as R . The equations for force and torque, with zero camber for a fixed inertial coordinate system, are

$$F_x = k_1 V_1 \cos(\theta) + k_2 V_2 \cos(120^\circ + \theta) + k_3 V_3 \cos(240^\circ + \theta) \quad (1)$$

$$F_y = k_1 V_1 \sin(\theta) + k_2 V_2 \sin(120^\circ + \theta) + k_3 V_3 \sin(240^\circ + \theta) \quad (2)$$

$$F_z = k_4 V_4 + k_5 V_5 + k_6 V_6 \quad (3)$$

$$M_x = k_4 V_4 R \cos(\theta) + k_5 V_5 R \cos(120^\circ + \theta) + k_6 V_6 R \cos(240^\circ + \theta) \quad (4)$$

$$M_y = k_4 V_4 R \sin(\theta) + k_5 V_5 R \sin(120^\circ + \theta) + k_6 V_6 R \sin(240^\circ + \theta) \quad (5)$$

$$M_z = k_1 V_1 R + k_2 V_2 R + k_3 V_3 R. \quad (6)$$

A. Mechanical Design

An instrumented wheel (SMART^{Wheel}) was made by modifying a Quickie mag wheel which consists of twelve pie-shaped sections. Three aluminum beams were designed and fabricated using EZ-CAM and a Bridgeport computer numerically controlled mill. The beams are mounted 120° apart on the wheel. Linear bearings were used so that force applied directly to the end of a beam (toward the hub) is transferred to the other two beams. The end of each beam was rounded to prevent pressing against the edge of the wheel. Each beam fits into the point of a pie-shaped wheel section. Slots in the gage area of the beams serve to increase surface strain and thus increase sensitivity. Each beam was secured at the hub while the push rim, via its standoffs, was mounted to the outer end of each beam.

B. Electronic Design

All beams were instrumented with one set of full strain gauge bridges (Micro-Measurements, EA-13-062AQ-350, 350 ohm foil strain gauges) with dc excitation for a total of three separate channels on the wheel. Circuitry designed and built on three pie-shaped printed circuit boards, one for each channel, were mounted into the sections of the wheel adjacent to the beams. The circuitry performs signal conditioning, filtering, and amplification for each channel.

The circuit board for each of the three channels on the wheel utilizes an AD1B31AN strain gauge signal conditioner chip to provide the excitation voltage to the strain gauge bridge, balance the bridge, amplify, and filter the signal. The excitation voltage is set to 9 V dc, the gain is adjustable between 500 and 1000, and the signal is low-pass filtered at 50 Hz.

A four-channel mercury slip-ring is used for signal transmission off the rotating wheel, with three lines carrying force signals and the other line serving as the reference ground line. A mercury slip-ring was selected over telemetry to minimize noise interference due to other laboratory test equipment. The three channels are then interfaced to an A/D board (DT 2825 and DT707) of a DOS-compatible 486 computer (33 MHz, 4 MBytes). A circular printed circuit board was designed to function as a slip-ring to bring power onto the wheel. Concentric copper traces on a circular PCB accept power from a ± 15 V commercial power supply via copper wipers. These wipers are mounted on the belt apparatus for the encoder. The ± 15 v power is then carried to on wheel boards each containing voltage regulators which create the required ± 12 supply voltages.

An optical encoder (Hewlett Packard, HEDS 5010) is used to detect the position of the beams with respect to top dead center. The digital position signal is converted to an analog signal and interfaced as a fourth channel to the AD board. The position of the beams and the channel signals are collected and saved into a Fine using double buffering DMA. A second program written with the ASYST software package is used to substitute the raw channel data and position data into equations which incorporate calibration constants and calculate the force components in the x and y directions and the moments 6 about the z axis. A third program is used to graphically display the force and torque data on the computer screen.

C. Software Design

Three programs were written with an ASYST software package. The ASYST package allows the programmer to configure the environment for the particular computer, data acquisition board, and specific application. The first program, COLLECT.TXT, reads the data from seven AD channels of the DT2825 and stores the data into a Fine. The second program, CONVERT.TXT, retrieves the data from the file, substitutes those voltage values and the calibration constants into equations which convert the channel data and position data to forces

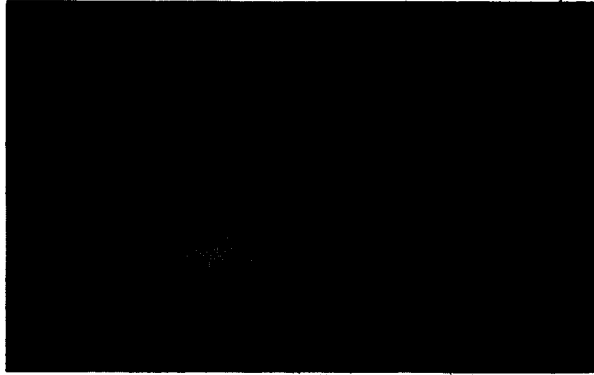


Fig. 2.

and torques, then stores the data to a new file. The third program, PLOT.TXT, graphically displays the force and torque data on the computer screen.

D. System Calibration and Testing

The three-channel wheel was calibrated with the wheel mounted vertically on a test stand via a wheelchair axle plate. Beam A was positioned at top dead center and weights were suspended from bottom dead center of the push rim. Measurements of the output voltage (at the output of the slip ring) were recorded for each of the three channels. Measurements were repeated with beam B at top dead center and again with beam C at top dead center. The voltage values recorded during the calibration procedure were substituted into the equation for F_y and used to solve for the calibration constants. Matlab was used to determine the calibration constants:

$$K_1 = 85.1525, K_2 = 84.5409, K_3 = 80.1959, R = 0.2794m.$$

These constants were later entered in the CONVERT.TXT program to convert the raw data to forces and torques. The system was characterized to determine its performance. Precision is 0.2 newtons. Resolution is two newtons. Linearity is 4.1% for the worst case. Correlation analysis showed the measured forces to be significantly correlated with the known forces ($r^2 = 1.0, p = .0001$). Accuracy was determined to be 4.1% for the worst case. The reproducibility is 1.5 newtons, which is within the resolution of the device. These measurements were made with the input range set to ± 125 newtons. The gain on the wheel's on-board amplifiers is adjustable as is the gain on the computer's analog to digital converter. Hence, these characteristics can be tuned for specific measurement applications. Previous experiments showed the accelerations of the wheelchair/rider system to be small and the inertia of the device was designed to be small [1]. The dynamic characteristics of the system were determined by spinning the wheel with no load on the pushrim at accelerations similar to normal wheelchair propulsion. Acceleration was recorded via the wheel's optical encoder. The wheel was spun on the calibration stand, and by having a subject push the wheel on a dynamometer without using the pushrim, by pushing on the tire. The measured inertia/acceleration components were determined to be negligible, i.e., within the resolution (2 N) of the device. However, as position, angular velocity, and angular acceleration are known, a computer program could be developed to minimize their effects.

TABLE I
SUBJECT PROFILES

Subject	Gender	Age (years)	Height	Weight (lbs.)	Nature of Disability	Wheelchair user?
DB	M	34	6'1.5"	160	Left leg Amputee	Yes
DP	M	28	5'10"	170	None	No
TC	M	42	5'9"	145	Post-polio	Yes
AV	F	39	5'4"	190	None	No
DS	M	33	6'1"	165	T-10 SCI	Yes
KA	F	27	5'4"	108	None	No
TS	M	30	5'6"	199	T-4 SCI	Yes
DH	M	25	5'10"	180	None	No
DV	M	23	5'10"	170	None	No
MF	F	24	5'4"	112	Limited right hand function	No

III. KINETIC AND KINEMATIC ANALYSIS OF WHEELCHAIR PROPULSION

Each of the ten individuals (three ambulatory men, three ambulatory women, and four male wheelchair users) gave informed consent to participate in this study. The etiology of the wheelchair users included two with paraplegia, one with postpolio, and one with a lower limb amputation. Each volunteer was asked to sit in a Quickie I wheelchair fitted with the three-channel wheel on its right side and secured to the CSUS dynamometer. The wheel camber was adjusted to zero degrees.

Markers (reflective stickers) were placed behind each subject's ear, on the back of the neck, on the shoulder, elbow, hip, knee, wrist, and knuckles for purposes of videotaping, digitizing, and correlating stroke kinematics. Markers were also placed on the top of the backrest, on the push rim at the point where it connects with beam A, and on the hub, for use in synchronizing the Kinetic data with the kinematic data.

Each subject was asked to propel the wheelchair at 1.34 to 1.79 m/s for three minutes for accommodation (Fig. 2). Each subject monitored his/her speed by viewing a digital tachometer mounted at the front of the dynamometer. At approximately two and one-half minutes, the video cameras were started (sagittal and frontal plane). At three minutes, the data collection program was started and lights were simultaneously illuminated to provide a signal on the videotape to indicate the beginning of data collection. Data were collected at 75 Hz per channel for approximately thirty seconds. Each subject then continued to propel himself/herself for at least fifteen seconds before the test was concluded.

A. Experimental Results

The gender, age, height, weight, and level of disability of each subject was recorded (Table I). Fig. 3 shows kinetic data for one revolution of the wheel for three subjects. The wheel top dead center position was determined by scanning the array (theta) containing the position data to find the index corresponding to the first reset to zero and the index corresponding to the point just prior to the next time the data reset to zero. Another program was used to extract the portion of data corresponding to the first full revolution of the wheel (starting from the first time during the data collection that the wheel hit top dead center) and to plot the F_x , F_y , and M_z curves on the screen and to a printer. The plots were examined and the position corresponding to the instant at which the torque (M_z) deviated from and the point

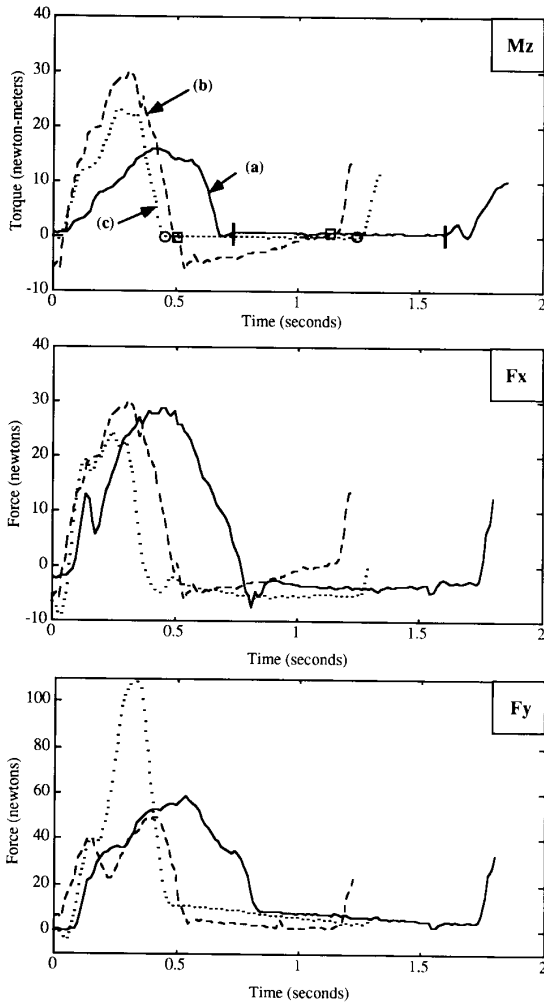


Fig. 3.

at which it returned to the baseline were recorded as the kinetic point of pushrim contact and point of pushrim release (Table II).

Videotape of the side view of the subjects was digitized using a Peak Technologies, Inc. Peak 2D Performance System. Frames were digitized beginning from the time at which the lights were activated. One image was skipped between every digitized frame. Markers on the hub and push rim were used to determine the first time the wheel hit top dead center and the first full revolution of the wheel. Stick figures of three subjects' first full stroke, within the data collection period, from point of contact to point of release are shown in Fig. 4. A protractor was used to measure the wheel positions corresponding to the point of pushrim contact and point of pushrim release. These values are given as the kinematic results in Table II.

IV. DISCUSSION

The results indicate that the 2D device tested provides kinetic information that temporally and spatially coincides with kinematic information gained through video analysis. One way analysis of variance of the kinetic and kinematic data showed no significant difference ($p < .05$) between the two methods for determining point of pushrim contact ($p < .84$) and point of pushrim release

TABLE II
ANGULAR POSITION OF BEAM A AT POINT OF
PUSHRIM CONTACT AND POINT OF RELEASE AS
DETERMINED FROM KINETIC AND KINEMATIC PLOTS

Subject	Point of Contact			Point of Release		
	Kinetic	Kinematic	Difference*	Kinetic	Kinematic	Difference*
DB	183°	180°	+3°	316°	313°	+3°
DP	170°	159°	+11°	247°	252°	-5°
TC	190°	185°	+5°	292°	292°	0°
AV	52°	49°	+3°	126°	125°	+1°
DS	29°	28°	+1°	113°	108°	+5°
KA	70°	67°	+3°	128°	138°	-10°
TS	166°	164°	+2°	252°	245°	+7°
DH	104°	94°	+10°	168°	167°	+1°
DV	101°	89°	+11°	202°	209°	-7°
MF	111°	110°	+1°	193°	186°	+7°

* Difference = kinetic - kinematic

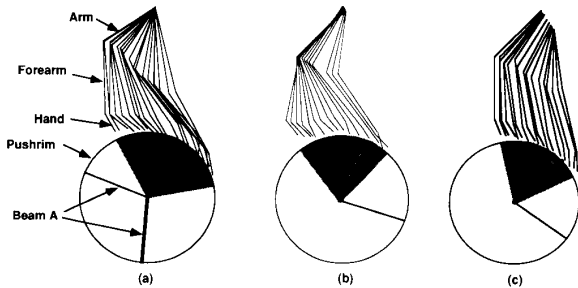


Fig. 4.

($p = .99$). Correlation analysis showed that results from kinetic and kinematic methods were significantly correlated ($p < .05$) for point of contact ($r^2 = .995, p = .0001$) and point of release ($r^2 = .993, p = .0002$). One way analysis of variance showed the angle of contact, point of contact minus point of release, were not significantly different ($p < .05$) when determined using kinetic or kinematic methods ($p = .62$). Correlation analysis showed the angle of contact to be significantly ($p < .05$) correlated for the two methods ($r^2 = .834, p = .0002$). There was some variation between the results of the two methods for individual subjects. However, the difference can be attributed to the accuracy with which the position could be measured from the plots and the resolution of the kinematic data. With the kinematic data, since only every other image was digitized, there were approximately one to five degrees of error. This error is proportional to the rotational speed of the wheel. Human error in digitizing the markers was also evident by the fact that there was variation in the hub location and distance between the hub and pushrim marker. This error was expected since the points are picked, frame by frame, using a cursor and a mouse. Error could be reduced by using a system which automatically digitizes the video information. It was also difficult to visually select the points of contact and release based on the digitized knuckle point. This was especially true for subjects who skimmed the pushrim during the recovery phase of the push cycle, this made it difficult to determine whether the hand was actually in contact with the rim or just covering it from the camera's view. It may have been advantageous to have concurrently analyzed video taken of the subject's front view to determine whether

the person was near the pushrim or actually grasping the pushrim. However, the ability to digitize in three-dimensional space was not available.

With preliminary results available, it is evident that there are points of interest that should be analyzed and further investigated in future studies. According to the kinematic data, most of the subjects appeared to be pushing smoothly. However, the kinetic data sometimes indicated otherwise. Some subjects exhibited an impact spike in the F_y curve which should be targeted for further analysis. The occurrence of double peaks in the force curves for some subjects also warrants further investigation. Most of the subjects imparted retarding forces in the negative x direction during portions of the push cycle. The manifestation of these forces and their effects should be explored as they could potentially have negative effects on propulsion efficiency and performance. The relatively large variation in peak force and torque values across subjects also suggests an area that should be examined in future studies. It was noticed that the magnitude of the force did not necessarily correspond with ability. For example, one of the female subjects who had difficulty maintaining a three mph speed, even while maintaining a higher stroke frequency, applied the largest F_y force in contrast to her low M_z . A thorough analysis must explore the proper fit of the wheelchair in terms of seat height and width, especially for women subjects.

REFERENCES

- [1] R. A. Cooper, "A force/energy optimization model for wheelchair athletics," *IEEE Trans. Syst., Man, and Cybern.*, vol. 20, pp. 444-449, 1990.
- [2] A. Vosse, R. Cooper, and B. Dhaliwal, "Computer control of a wheelchair dynamometer," in *Proc. RESNA 13th Annu. Conf.*, Washington, DC, pp. 59-60, 1990.
- [3] R. A. Cooper and A. Cheda, "Measurement of racing wheelchair propulsion torque," in *Proc. IEEE-EMBS 11th Int. Conf.*, vol. 11, pp. 530-531, 1989.
- [4] R. A. Cooper, "An exploratory study of racing wheelchair propulsion dynamics," *Adapt. Phys. Act. Q.*, vol. 7, pp. 74-85, 1990.
- [5] R. A. Cooper, "A systems approach to the modeling of racing wheelchair propulsion," *J. Rehabil. Res. Dev.*, vol. 27, no. 2, pp. 151-162, 1990.
- [6] R. A. Cooper, "Wheelchair racing sports science: A review," *J. Rehabil. Res. Dev.*, vol. 27, no. 3, pp. 295-312, 1990.
- [7] L. H. V. Van Der Woude, H. E. I. Veeger, and R. H. Rozendal, "Propulsion technique in handrim wheelchair ambulation," *J. Med. Eng. Tech.*, vol. 13, no. 1/2, pp. 136-141, 1989.
- [8] C. E. Brubaker, C. A. McLaurin, I. D. Gibson, and T. H. Soos, "Seat position and wheelchair performance," *Wheelchair Mobility 1976-1981*, W. Stamp, and C. A. McLaurin, Eds. Rehabilitation Engineering Center, University of Virginia, pp. 12-21, 1981.
- [9] S. A. Ross and C. E. Brubaker, "Electromyographic analysis of selected upper extremity muscles during wheelchair propulsion," in *Proc. 2nd Int. Conf. Rehabil. Eng.*, pp. 7-8, 1984.
- [10] W. Lesser, "Ergonomische Untersuchung der Gestaltung antriebsrelevanter Einflussgrößen beim Rollstuhl mit Handantrieb," *Fortschrittberichte VDI Verlag*, Reihe 17, Biotechnik No. 28, p. 265, 1986.
- [11] S. I. Tupling, G. M. Davis, M. R. Piernynowski, and R. I. Shephard, "Arm strength and impulse generation: Initiation of wheelchair movement by the physically disabled," *Ergonomics*, vol. 29, pp. 303-311, 1986.
- [12] R. L. Brauer and B. A. Hertig, "Torque generation on wheelchair handrims," in *Proc. 1981 Biomechanics Symp., ASME/ASCE Mechanics Conf.*, pp. 113-116, 1981.
- [13] C. E. Brubaker, S. Ross, and C. A. McLaurin, "Effect of seat position on handrim force," in *Proc. 5th Annu. Conf. Rehabilitation Engineering*, p. 111, 1982.
- [14] M. G. Strauss, I. Maloney, F. Ngo, and M. Phillips, "Measurement of the dynamic forces during manual wheelchair propulsion," in *Proc. Am. Soc. Biomechanics 15th Annu. Meeting*, pp. 210-211, 1991.
- [15] M. G. Strauss, M. H. Moeinzadeh, M. Schneller and I. Trimble, "The development of an instrumented wheel to determine the handrim forces during wheelchair propulsion," in *Proc. ASME Winter Annu. Meeting*, pp. 53-54, 1989.
- [16] K. T. Watanabe, R. A. Cooper and I. F. Ster III, "SMARTWheels: A device for studying wheelchair propulsion dynamics," in *Proc. IEEE-EMBS 13th Int. Conf.*, vol. 13, no. 4, pp. 1817-1818, 1991.

Magnetic Resonance Imaging Can Cause Focal Heating in a Nonuniform Phantom

Peter L. Davis, Charles Shang, Lalith Talagala, and A. William Pasculle

Abstract—To test if the radiofrequency fields of a magnetic resonance imager could cause focal heating, two cylindrical phantoms were made from a mixture of agar and saline. The first phantom was uniform; the second was nonuniform in that a narrow bridge of agar was produced. Both phantoms were exposed to high levels of radiofrequency power (140 W) at 63 MHz and the temperature rises were measured. In the uniform phantom, the temperature increased as the radius increased. In the bridge phantom, the narrow bridge heated three times greater than at the opposite uniform periphery, and over five times the average of the uniform phantom.

This experiment demonstrates that the radiofrequency fields of magnetic resonance imagers can cause focal heating if the exposed object is nonuniform. Since nonuniformity is present in the human body, as the radiofrequency power of magnetic resonance imaging techniques increases, focal heating in patients is a concern.

I. INTRODUCTION

The radiofrequency (RF) fields in magnetic resonance imaging (MRI) are known to cause heating. Extensive human and animal research has been performed to show that RF energy deposited by standard MRI examinations appears to pose no potential human health hazards [1]-[5]. However, new imaging techniques such as magnetization transfer contrast and rapid acquisition with relaxation enhancement have the potential to significantly increase the amount of RF energy deposited in the body [6], [7].

In general, the research experiments have utilized cutaneous or subcutaneous temperature measurements. These measurements have been considered adequate since, according to theory for a homogeneous object, greater current induction and therefore greater heating will occur at the periphery as opposed to the center of the object [8]-[10]. However, the body is not a uniform electrical conductor. Organ shapes and highly resistive fat planes can alter the paths of the induced electrical currents. In theory, this alteration of the current path can lead to focal heating [11]-[12]. Computer modeling of the human body using parameters consistent with MR imagers operating at 63 MHz had demonstrated that substantial focal heating may potentially occur in the paraspinal muscles [11], [12]. In this study, we experimentally verify this using phantoms exposed in a clinical MR imager.

Manuscript received February 24, 1992; revised May 1993.

P. L. Davis, C. Shang, and L. Talagala are with the Department of Radiology, the University of Pittsburgh Medical Center, Pittsburgh, PA 15213.

A. W. Pasculle is with the Department of Microbiology, University of Pittsburgh Medical Center, Pittsburgh, PA 15213.

IEEE Log Number 9213163.